New Journal of Physics
The open access journal for physics

# Interactions of membranes with coarse-grain proteins: a comparison

**Jörg Neder**[1], **Peter Nielaba**[1], **Beate West**[2] **and Friederike Schmid**[3,4]

[1] Department of Physics, University of Konstanz, Germany
[2] Department of Physics, University of Bielefeld, Germany
[3] Institute of Physics, University of Mainz, Germany
E-mail: friederike.schmid@uni-mainz.de

*New Journal of Physics* **14** (2012) 125017 (24pp)
Received 1 June 2012
Published 31 December 2012
Online at http://www.njp.org/
doi:10.1088/1367-2630/14/12/125017

**Abstract.** We study the interactions between lipid bilayers and rigid transmembrane proteins by Monte Carlo simulations of generic coarse-grain models. Different popular protein models are considered and compared with each other, and key parameters such as the hydrophobicity and the hydrophobic mismatch are varied systematically. Furthermore, the properties of the membrane are manipulated by applying different tensions. The response of the membrane to the insertion of single proteins is found to be mostly generic and independent of the choice of the protein model. Likewise, the orientational distributions of single proteins depend mainly on the hydrophobic mismatch and the hydrophobicity of the proteins, and are otherwise similar for all protein models. Orientational distributions are generally found to be very broad, i.e. tilt angles fluctuate very much, in agreement with experimental findings. Weakly hydrophobic proteins respond to positive hydrophobic mismatch by tilting. Strongly hydrophobic (strongly bound) proteins distort the surrounding membrane and tend to remain upright. For proteins with intermediate hydrophobicity, the two mechanisms compete, and as a result, the tilt only sets in if the hydrophobic mismatch exceeds a threshold. Clusters of several strongly hydrophobic proteins with negative positive mismatch may nucleate raft-like structures in membranes. This effect is more pronounced for proteins with rough, structured surfaces.

[4] Author to whom any correspondence should be addressed.

## Contents



## 1. Introduction

Biological membranes are a central component of all living creatures [1, 2]. They are used to create compartments, to enclose substances and to control and regulate transport processes and signaling. All biomembranes have the same basic structure, i.e. a self-assembled phospholipid bilayer. Their individual properties and functionalities depend on the specific lipid content and, most importantly, on the associated set of membrane proteins. On average, proteins constitute 50% of the membrane mass, as in plasma membranes or exterior membranes. Relatively pure lipids with a low protein content of only about 18% are found around certain nerve fibers. In contrast, energy-transduction membranes have a very high content of proteins, typically around 75% [3].

Nowadays, our picture of biomembranes is based on the 'fluid mosaic model' of Singer and Nicolson [4, 5], according to which the lipid membranes of biological cells are in a dynamic fluid state in which proteins are free to move around. The proteins themselves are basically found to be peripheral proteins that are only loosely attached to the membrane surface and integral membrane proteins that cannot be easily separated from the lipids. The latter type forms the major fraction of membrane proteins [6]. In their original 1972 model [4], Singer and Nicolson assumed that proteins and lipids diffuse freely and that the membrane structure on larger scales is largely homogeneous as a result. More recent experimental results suggest that the distribution of proteins in the membrane is in fact heterogeneous [5, 7] and that some membrane proteins can be transiently trapped in certain membrane areas [8–12]. The mechanisms governing this lateral compartmentalization—whether it is driven by lipids or proteins—are still under debate. For example, the popular 'raft hypothesis' assumes that the driving mechanism is nanodomain formation in the underlying lipid matrix, which may be stabilized by lipid–protein interactions [13, 14]. However, the nature of the rafts, and even the question of whether they really do exist *in vivo*, is still being discussed controversially [15].

The complexity of natural membranes makes it necessary to investigate simplified model bilayers which are composed of one or two different lipid species. Understanding the

physical principles that govern the dynamic and structural behavior of these model membranes is the aim of a large number of both experimental as well as theoretical studies [16]. Unfortunately, structural perturbations or transformations of the lipid bilayer in the presence of proteins are among the most difficult processes to probe experimentally [17]. Thus, complementary theoretical approaches and computer simulations of membrane systems of well-defined compositions are necessary to elucidate the role of the lipid bilayer in processes such as protein aggregation and function. Depending on the length and time scales of interest, a variety of computational methods and models have been developed [16, 18, 19]. Microscopic studies in atomistic detail are restricted to relatively small system sizes, and the proteins are surrounded by only a relatively small ring of lipids in most simulations. To study the long-range influence of proteins on lipid bilayers, coarse-grained approaches are necessary [16, 20]. These allow one to study generic aspects of lipid–protein interactions on larger scales, for example, the distortion of the lipid bilayers due to the presence of lipids [16, 21]. This problem has also been considered by various theoretical approaches, ranging from molecular mean-field theories [22–26], to elastic continuum theories [27–36]. In all these studies, the integral proteins were represented by simplified objects, either as smooth cylinders (this representation is usually used in theoretical approaches) or as rigid objects made of beads (the most common approach in coarse-grained simulations [34, 37–40]). Such simplifications are based on the idea that generic aspects of membrane–protein interactions should not depend on the microscopic details of the protein structure. However, since even simplified objects, of course, have a microscopic structure (e.g. the structure of a smooth surface), it is not *a priori* clear which simulation results are generic and which are a specific property of the chosen model. So far, systematic comparisons of different protein models are lacking.

The present study attempts to close this gap. We compare the response of lipid bilayers to the insertion of different 'protein'-like inclusions, namely two variants of bead proteins and smooth spherocylinders. Key parameters such as the hydrophobic length of the inclusion and the strength of the hydrophobic interaction are varied systematically. Moreover, we also consider different fluid membrane states, i.e. tensionless membranes and membranes subject to a strong tension. Previous studies have shown that the internal structure of membranes changes under tension [41]. The monolayers are less well separated and one has a significant amount of interdigitation. Varying the tension, thus, allows us to assess the influence of the local lipid structure on the lipid–protein interactions.

Our study is based on a generic molecular membrane model [42, 43], which has been shown to reproduce the main phases and phase transitions of single component phospholipid bilayers, including the high-temperature fluid phase $L_\alpha$, the low-temperature tilted gel phase $L_{\beta'}$ and the intermediate ripple phase $P_{\beta'}$ [43]. Moreover, the elastic properties of the membranes (such as the bending stiffness, area compressibility, etc) were found to be in semiquantitative agreement with those of bilayers made of dipalmitoylphosphatidylcholine (DPPC), which is one of the most abundant lipids in real biomembranes [44]. In previous work, we have investigated the membrane-mediated effective interactions between smooth cylindrical inclusions, either of infinite [41, 44, 45] or of finite length [45] in these model membranes. Here we will focus on the protein–lipid interactions and on the comparison of different protein models. We mainly consider single inclusions, but we will also discuss clusters of inclusions in the end.

## 2. Models and method

### 2.1. Lipid bilayer

In this section, we will first briefly summarize our lipid model and then introduce the different protein models studied in this work. The lipid model was originally introduced in the context of Langmuir monolayers [46–48], and was shown to reproduce the generic phase behavior of fatty acid monolayers in the practically relevant region of the transition between the liquid expanded and the liquid condensed region [48]. Combined with a suitable, computationally cheap solvent model [49], it can also be used to study self-assembled lipid bilayers and their main phase transitions [42, 43, 50]. Lipids are represented by a linear chain of $n$ tail beads (t) of diameter $\sigma_t$, attached to one slightly larger head bead (h) with a diameter of $\sigma_h$. They are immersed in solvent beads (s) of diameter $\sigma_s$. Within lipid chains, beads are connected by a finite extensible nonlinear elastic (FENE) bond potential

$$V_{\mathrm{FENE}}(r) = \begin{cases} -\frac{\epsilon_{\mathrm{FENE}}}{2}(\Delta r_{\max})^2 \ln\left(1 - \left(\frac{r-r_0}{\Delta r_{\max}}\right)^2\right) & \text{if } |r - r_0| < \Delta r_{\max}, \\ \infty & \text{otherwise.} \end{cases} \tag{1}$$

Here $r_0$ denotes the equilibrium length of the bond and $\Delta r_{\max}$ the maximal deviation, i.e. subsequent beads within a chain cannot come closer than $r_0 - \Delta r_{\max}$ or be pulled further apart than $r_0 + \Delta r_{\max}$. The angle $\theta$ between subsequent bonds in the lipid gives rise to a stiffness potential

$$V_{\mathrm{BA}}(\theta) = \epsilon_{\mathrm{BA}}(1 + \cos\theta)\,. \tag{2}$$

Beads that are not directly adjacent in the same chain interact through a truncated and shifted Lennard-Jones (LJ) potential.

$$V_{ij}(r) = \begin{cases} V_{\mathrm{LJ}}(r/\sigma_{ij}) - V_{\mathrm{LJ}}(r_{\mathrm{c},ij}/\sigma_{ij}) & \text{if } r < r_{\mathrm{c},ij}, \\ 0 & \text{otherwise,} \end{cases} \tag{3}$$

with

$$V_{\mathrm{LJ}}(r) = \epsilon\left(\frac{1}{r^{12}} - 2\frac{1}{r^6}\right). \tag{4}$$

The parameter $\sigma_{ij} = (\sigma_i + \sigma_j)/2$ is the arithmetic mean of the diameters $\sigma_i$ of the interaction partners, and $r_{c,ij} = 1\,\sigma_{ij}$ for all partners $(ij)$ except $(tt)$ and $(ss)$: $r_{c,tt} = 2\,\sigma_{tt}$ and $r_{c,ss} = 0$. Hence tail beads attract one another, all other interactions are repulsive, and solvent beads do not interact at all with each other. The solvent outside the lipid bilayer behaves like an ideal gas fluid and has no internal structure. In the presence of solvent, the model lipid chains self-assemble spontaneously into bilayers.

Specifically, we use the model parameters [42] $n = 6$ (i.e. the lipid chains comprise seven beads in total), $\sigma_h = 1.1\,\sigma_t$, $\sigma_s = \sigma_h$, $r_0 = 0.7\,\sigma_t$, $\Delta r_{\max} = 0.2\,\sigma_t$, $\epsilon_{\mathrm{FENE}} = 100\,\epsilon/\sigma_t^2$ and $\epsilon_{\mathrm{BA}} = 4.7\,\epsilon$, and we work at a nominal pressure of $P = 2.0\,\epsilon/\sigma_t^3$. As already mentioned in the introduction, the model reproduces the main phases of phospholipids, i.e. a high-temperature fluid $L_\alpha$ phase at temperature $k_B T > k_B T_m \sim 1.2\,\epsilon$ and a low-temperature tilted gel ($L_{\beta'}$) with an intermediate modulated ripple ($P_{\beta'}$) phase [43]. The energy and length scales can be mapped to SI units [44] by matching the bilayer thickness or, alternatively, the area per lipid and the temperature of the main transition to those of DPPC, giving $1\,\sigma_t \sim 6$ Å and $1\,\epsilon \sim 0.36 \times 10^{-20}$ J.

The elastic material properties of the membranes in the fluid state were found to be comparable to those of DPPC membranes [44].

### 2.2. Protein models

All known integral membrane proteins are either composed of $\alpha$-helices forming helical bundle proteins or $\beta$-strands, which produce $\beta$-barrel proteins. This has motivated generic models where integral proteins are represented by hydrophobic cylinders or cylinder assemblies.

The interaction strength between the hydrophobic core of the membrane and the hydrophobic part of the inclusion crucially influences the local perturbation of the bilayer. Since hydrophobic interaction does not arise from the binding of nonpolar molecules to each other, but from preventing polar solvent molecules from achieving optimal hydrogen binding, the strength of the hydrophobic interaction depends on the relative polarity of both the solute and the solvent [51]. Experimentally, the hydrophobicity of proteins can therefore be tuned by changing amino acid residues with different hydrophobicities of the protein [52]. As an example, alanine is less hydrophobic than leucine [53]. Alternatively, changing the pH of the solvent and thereby changing the ion dissociation on side chains will also affect the hydrophobic interaction of the lipid bilayer and the proteins [54].

A second critical parameter is the hydrophobic length of the protein, i.e. the length of the hydrophobic section on the protein, compared to the hydrophobic thickness of the membrane. In the case of 'hydrophobic matching', the hydrophobic length of any transmembrane domain matches the hydrophobic thickness of the bilayer [55]. If the thickness of the hydrophobic core of the unperturbed bilayer is larger than the hydrophobic length of the protein, one has 'negative mismatch', and if the hydrophobic length of the protein surmounts the bilayer thickness, one has 'positive mismatch'. Hydrophobic mismatch can have various consequences for proteins, such as tilt or conformational changes of transmembrane parts, lateral oligomerization or even failure of membrane insertion [32]. Furthermore, it may also influence the properties of the lipids [56, 57]. The lipid chain order may be changing, the phase transition temperature can be modified, the formation of microdomains is possible or even nonlamellar structures may be induced.

Here we compare three different models for simple transmembrane proteins. All have a hydrophobic middle section, i.e. a section which attracts tail beads. The length of this section and the strength of the hydrophobic interactions can be tuned. A picture of the three models is shown in figure 1.

The first type of model protein is a smooth spherocylinder with a hydrophobic length $L$, capped at both ends by effectively repulsive ('hydrophilic') hemispheres [45] (figure 1, left). It is parameterized by a line of length $L$. The interactions between proteins and lipids or solvent beads have a repulsive contribution

$$V_{\mathrm{rep}}(r) = \begin{cases} V_{\mathrm{LJ}}\left(\frac{r-\sigma_0}{\sigma}\right) - V_{\mathrm{LJ}}(1) & \text{if } r - \sigma_0 < 0, \\ 0 & \text{otherwise,} \end{cases} \tag{5}$$

where $r$ denotes the shortest distance between the protein line and the center of the bead, $\sigma$ is given by $\sigma = (\sigma_{\mathrm{t}} + \sigma_i)/2$ for interactions with beads of type $i$ ($i = h, t$ and $s$ for the head, tail and solvent beads, respectively), $\sigma_0 = \sigma_{\mathrm{t}}$ and $V_{\mathrm{LJ}}$ has been defined above (equation (4)). In addition, tail beads are attracted to the straight inner section of the protein by an attractive potential that

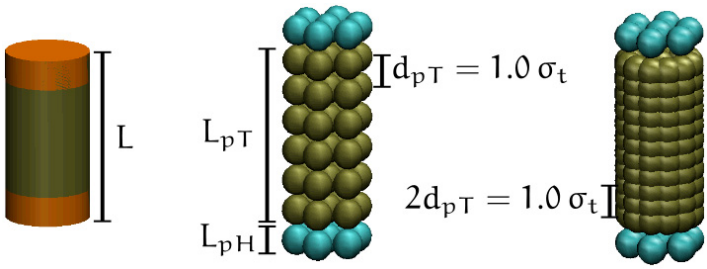


**Figure 1.** Protein models considered in this work. Left: a smooth spherocylinder. Middle: rough bead protein. Right: smooth bead protein. Bead proteins (middle and right) are characterized by their hydrophobic and hydrophilic lengths $L_{pT}$ and $L_{pH}$ and their level of corrugation $d_{pT}$.

depends on the projection of the distance $d$ between the centers of the tail bead and the protein onto the protein axis. The total potential for tail beads reads

$$V_{pt}(r, d) = \frac{\epsilon_{pt}}{\epsilon}\left(V_{rep}(r) + V_{attr}(r) \times W_P(d)\right), \tag{6}$$

with the attractive Lennard-Jones contribution

$$V_{attr} = \begin{cases} V_{LJ}(1) - V_{LJ}(2) & \text{if } r - \sigma_0 < \sigma, \\ V_{LJ}\left(\frac{r-\sigma_0}{\sigma}\right) - V_{LJ}(2) & \text{if } \sigma < r - \sigma_0 < 2\sigma, \\ 0 & \text{otherwise,} \end{cases} \tag{7}$$

and a weight function $W_P(d)$, which is unity on a stretch of length $2l = L - 2\sigma_t$ and crosses over smoothly to zero over a distance of approximately $\sigma_t$ at both sides. Specifically, we use

$$W_P = \begin{cases} 1 & \text{if } |d| \leqslant l, \\ \cos^2\left(\frac{3}{2}(|d| - l)\right) & \text{if } l < |d| < l + \frac{\pi}{3}, \\ 0 & \text{otherwise.} \end{cases} \tag{8}$$

The hydrophobicity of the protein can be tuned by varying the parameter $\epsilon_{pt}$. In systems containing several proteins, the direct protein–protein interactions are purely repulsive and have the form of equation (5) with $\sigma = \sigma_t$, $\sigma_0 = 2\sigma_t$ and $r$ the minimum distance between the two protein lines.

In our own previous work [41, 44, 45], we used a restricted variant of this model, where the cylinders had infinite length (albeit with a finite hydrophobic section $L$) and fixed orientation in the direction normal to the membrane. This corresponds to the situation most commonly considered in theories of protein-induced bilayer distortions. Here we focus on more realistic simulation models and study cylinders with full orientational freedom. Representing a complex structure like a protein by a compact cylindrical object might seem a rather crude approach. However, this can be justified by the fact that, e.g., $\alpha$-helices are packed with very little free space within the helices [58] and are therefore fairly smooth on the scale of $\sim$10 Å. There are no large cavities into which chains or even whole molecules would fit [59].

The other two protein models have surfaces of varying roughness. The second type of model protein, which we will call 'rough bead protein' in the following, consists of hydrophobic ($pT$) and hydrophilic ($pH$) beads having the same diameter as the tail beads, i.e. $\sigma_{pT} =$

$\sigma_{pH} = 1\,\sigma_t$. This way of modeling proteins is common in coarse-grained simulation studies of membrane–protein interactions [34, 35, 37–40]. Specifically, the proteins are constructed as rigid stacks of discs separated by a distance $d_{pT} = \sigma_t$. Each disc consists of an outer ring of $N_p$ beads with the nearest-neighbor distance $d_{pT}$, which is filled with further beads if necessary. The diameter $D_p$ of the protein is therefore given by

$$D_p = \frac{d_{pT}}{\sin(\Delta\alpha_p/2)} + \sigma_{pT} = \frac{d_{pT}}{\sin(\pi/N_p)} + \sigma_{pT}. \tag{9}$$

One disc of hydrophilic beads is added at each end of the protein. Hence, the total length of a bead protein is $L = L_{pT} + 2L_{pH}$, where $L_{pT}$ sets the hydrophobic length (see figure 1, middle). The hydrophobicity of the protein can be tuned with the interaction parameter $\epsilon_{pTt}$ governing the strength of the attractive interactions between hydrophobic protein and lipid beads. Beads within one protein are rigidly ordered and do not have any additional degrees of freedom. In comparable dissipative particle dynamics (DPD) simulations where protein beads were connected by springs, no appreciable internal deformation of the proteins was observed, except for a slight bending of very slim proteins [38].

Compared to the smooth spherocylinder, the surface structure of the rough bead proteins is rather corrugated. Our third model protein, which we denote by 'smooth bead protein' is constructed as an intermediate model with reduced corrugation. This is achieved by doubling the number of beads and reducing the minimum separation to $d_{pT} = 0.5\,\sigma_t$. To obtain hydrophobic interaction strengths that are comparable to the rough bead protein model, the interaction parameter $\epsilon_{pTt}$ has to be rescaled. The rescaled parameters will be marked as $\tilde{\epsilon}$ in the following. As a first estimate, simple geometrical considerations suggest that a rescaled energy of $\tilde{\epsilon}_{pTt} = 0.25\,\epsilon$ should lead to similar behavior of the smooth bead protein as $\epsilon_{pTt} = 1.0\,\epsilon$ for the rough bead protein.

In this paper, we will discuss proteins of diameter $D_p \sim 3\sigma_t$, corresponding to the diameter of a $\beta$-helix such as, e.g., gramicidine [44]. Thus our rough bead proteins contain $N_p = 6$ beads per disc, and the smooth bead proteins contain $N_p = 12$ beads per disc (cf figure 1). We have also studied proteins with smaller diameter (down to $D_p \sim 1\sigma_t$, corresponding to an $\alpha$-helix) and larger diameter (up to $D_p \sim 5\sigma_t$). The results were qualitatively similar and will not be shown here. Details can be found in the theses [60, 61].

### *2.3. Simulation method*

The systems described above were studied by Monte Carlo simulations at constant pressure, constant temperature $T = 1.3\epsilon/k_B$, constant pressure $P = 2.0\epsilon/\sigma_t^3$ and constant surface tension $\Gamma$ (with $\Gamma = 0$ unless stated otherwise) in a simulation box of variable size and shape. Following [62], we impose tension via an additional energy term $-\Gamma A$ in the Hamiltonian of the system, where $A$ is the projected area of the bilayer onto the $xy$-plane. The noninteracting solvent particles, which probe the free volume and force the lipids to self-assemble, are not affected by this additional energy contribution. They ensure that the normal pressure $P_N$ is kept fixed at the required value. Thus, we are performing Monte Carlo simulations in the $NP_N\Gamma T$ ensemble with the effective Hamiltonian

$$H_{eff} = U + P_N V - \Gamma A - Nk_B T \ln(V/V_0), \tag{10}$$

where $U$ is the interaction energy, $V$ the volume of the simulation box, $V_0 = \sigma_t^3$ our reference volume and $N$ the total number of beads (cf [42]). We use three main types of Monte Carlo

moves, namely (i) local moves of lipid or solvent beads, (ii) global moves which change the size or shape of the simulation box and involve rescaling of all particle coordinates [42] and (iii) protein rotation or translation moves [45]. The moves are proposed randomly and accepted according to a Metropolis criterion. In each Monte Carlo sweep (MCS), every bead is moved once on average and the protein is moved and rotated once. The computationally expensive global rescaling moves were attempted every 50th MCS.

The system sizes ranged from ∼780 lipids and ∼12 300 solvent beads for the thin proteins to ∼1640 lipids and ∼24 600 solvent beads for the thickest proteins. Typical run lengths were of the order of several million MCS with equilibration times of up to one million MCS.

## 3. Results: single proteins

In this section, we compare the interactions between lipid membranes and single proteins for our three different protein models. Since the direct interactions between the proteins and the lipid molecules are rather different in the three models, the direct quantitative comparison is nontrivial. To set the stage from a thermodynamic point of view, we first consider the free energies of protein insertion for the different models. Then we discuss the influence of the proteins on the surrounding lipid bilayer, and finally, the orientational distributions of the proteins.

### *3.1. Binding free energies*

The effective binding energy of the proteins to the membrane can be determined from the Gibbs free energies of insertion. In our context, the quantity of interest is the difference $\Delta G_{\mathrm{eff}} = \Delta G - \Delta G_{\mathrm{s}}$ between the Gibbs free energy of inserting a protein in a membrane and the Gibbs free energy of inserting a protein in a pure solvent. To determine $\Delta G$ and $\Delta G_{\mathrm{s}}$, we use a variant of the Widom insertion method [63] and gradually insert the protein by modifying its interaction potentials with a parameter $\lambda$. At $\lambda = 0.0$ the interaction must vanish completely and at $\lambda = 1.0$ it reaches its full interaction strength. The difference in Gibbs energy $\Delta G$ can then be calculated by thermodynamic integration,

$$\Delta G = \int_0^1 \left\langle \frac{\partial H}{\partial \lambda} \right\rangle_\lambda \mathrm{d}\lambda. \tag{11}$$

The derivative $\partial H/\partial\lambda$ can be calculated analytically and its value is recorded similarly to the other observables during the simulation.

For the smooth cylinders, we replaced the total interaction energy $U_{\mathrm{ip}}$ between the protein and lipids or solvent by a rescaled energy

$$\tilde{U}_{\mathrm{ip}}(\vec{r}^N, \lambda) = -\ln(1 + \lambda(\mathrm{e}^{-U_{\mathrm{ip}}(\vec{r}^N)} - 1)). \tag{12}$$

At low values of $\lambda$, this potential is not sufficient to bind the proteins to the membrane, which results in sampling problems. Therefore, we used a restricted model where the protein cylinders had infinite length (but finite hydrophobic portion $L$) and thus stay in the membrane by construction [44]. Here, 'infinite length' means that the cylinder extends through the whole simulation box and is connected by the periodic boundary conditions, which implies that it cannot tilt.

In the case of the bead proteins, the interaction potentials are all of Lennard-Jones type and we can follow the approach of Beutler *et al* [64]: the modified interaction energy between the

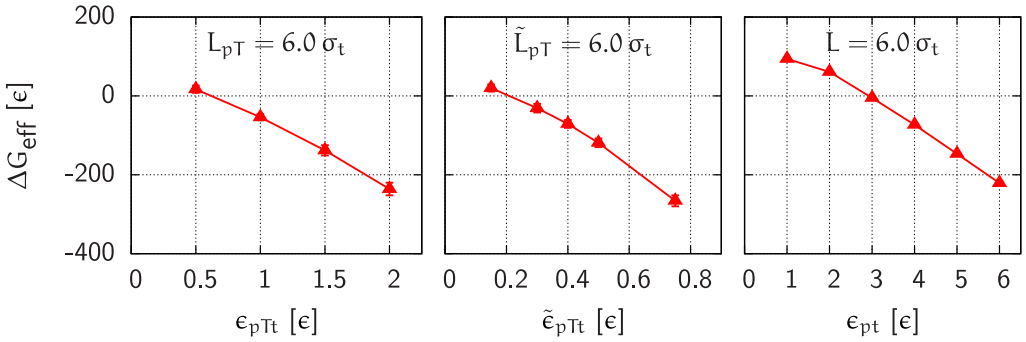


**Figure 2.** Effective free energy of binding the three types of protein to a tensionless membrane versus hydrophobicity. Left: rough bead protein. Middle: smooth bead protein. Right: a cylinder. The hydrophobic length of all proteins is $6\sigma_t$. Lines are a guide to the eye.

beads of the gradually inserted protein $k$ and the (unaltered) beads of the lipids and the solvent $i$ at distance $r_{ki}$ reads

$$\Phi_{ki,\lambda} = \epsilon_{ki}\lambda^n \left( \frac{1}{[\alpha_{\mathrm{LJ}}(1-\lambda)^2 + (r_{ki}/\sigma_{ki})^6]^2} - \frac{2}{\alpha_{\mathrm{LJ}}(1-\lambda)^2 + (r_{ki}/\sigma_{ki})^6} \right) + \Phi_{ki,\lambda,\mathrm{cutoff}}, \tag{13}$$

where $\Phi_{ki,\lambda,\mathrm{cutoff}}$ is set such that the potential is continuous at the cutoff radius $r_{ki,\mathrm{c}}$. In the case of purely repulsive soft-core potentials, the cutoff radius is also shifted to

$$r_{ki,\lambda,\mathrm{min}} = \sqrt[6]{1-\alpha(1-\lambda)}\sigma_{ki} \tag{14}$$

in order to account for the shift of the local minimum of the modified Lennard-Jones potential. The values of $n$ and $\alpha_{\mathrm{LJ}}$ can be tuned such that the proteins remain in the membrane for all values of $\lambda$. Good results were obtained with $n = 1$ and $\alpha_{\mathrm{LJ}} = 0.40$.

Figure 2 shows the results on the binding energies for different proteins with hydrophobic length $L = 6\sigma_t$. These proteins are 'hydrophobically matched'; therefore deformation of the bilayer is minimal (see the next subsection) and the binding energy results mainly from the competition between the interaction energy and the entropy loss associated with conformational changes in the lipid bilayer. The comparison of binding energies enables one to relate the interaction parameters in the different models with each other. Figure 2 shows that smooth bead proteins with hydrophobic interaction value $\tilde{\epsilon}_{\mathrm{p}T\mathrm{t}}$ have roughly the same binding energies as rough bead proteins with hydrophobic interaction value $\epsilon_{\mathrm{p}T\mathrm{t}} = 3\tilde{\epsilon}_{\mathrm{p}T\mathrm{t}}$ and cylinders with hydrophobic interaction value $\epsilon_{\mathrm{p}t} = 10\tilde{\epsilon}_{\mathrm{p}T\mathrm{t}}$. This relation will be further supported below when inspecting quantities such as the bilayer thickness or the director fields around cylindrical proteins and bead proteins, respectively.

The influence of the binding energies on the hydrophobic length of the protein is examined in figure 3 for the case of rough bead proteins. For a small hydrophobic strength $\epsilon_{\mathrm{p}T\mathrm{t}} = 0.5$, the binding energy is positive, $\Delta G_{\mathrm{eff}} > 0$; thus the protein does not bind at thermodynamic equilibrium. Nevertheless, it was possible to prepare metastable states where such weakly hydrophobic proteins span through a membrane, and these states mostly remained metastable during the whole simulation run. Only proteins with a small hydrophobic length $L_{\mathrm{p}T} = 4\sigma_t$ were occasionally expelled out of the membrane. The transmembrane state is stabilized by a high kinetic barrier, created by the fact that the hydrophilic caps have to traverse the hydrophobic

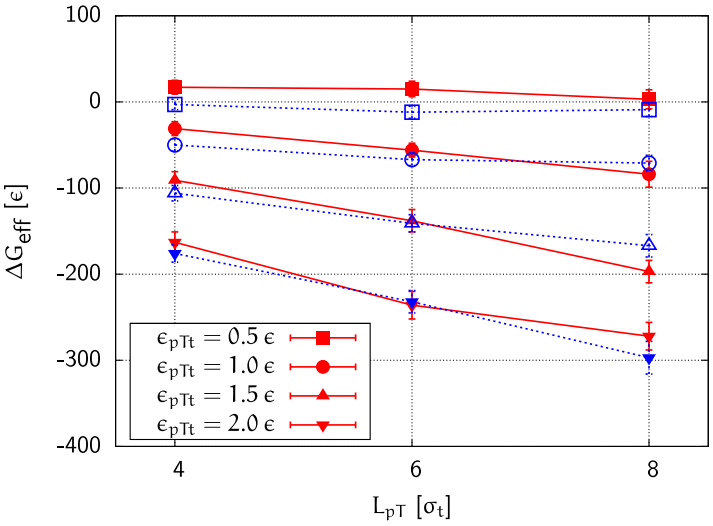


**Figure 3.** Effective free energy of binding a rough bead protein to a tensionless membrane versus hydrophobic length $L_{pT}$ for different hydrophobicities $\epsilon_{pTt}$ as indicated. Full symbols connected by solid lines mark the results for tensionless membranes, and open symbols connected by dashed lines the results for membranes under a tension $\Gamma = 2.0\,\epsilon/\sigma_t^2$. Lines are a guide to the eye.

core of the membrane during an expulsion process. A related observation was made by Illya and Deserno [65] in a recent study of peptide-induced pore formation. They report that at a certain peptide–lipid attraction, proteins initially placed above the bilayer bound to the upper monolayer, but did not insert. If the same peptide was initially placed inside the bilayer with its long axis parallel to the bilayer normal, it remains in the bilayer.

The 'binding energies' in the nonbinding regime do not depend on the hydrophobic length $L_{pT}$ of the protein. As soon as the protein binds, however ($\Delta G_{eff} < 0$), the binding energy decreases with increasing $L_{pT}$. Figure 3 also shows binding energies in membranes under the tension $\Gamma = 2\epsilon/\sigma_t^2$. The trends are similar and even the values are comparable.

### *3.2. Bilayer distortion close to proteins*

Next we investigate the effect of the protein on the surrounding lipid bilayer. One particularly pronounced phenomenon is the distortion of the membrane thickness in the vicinity of the proteins. This is shown for the different protein models in figure 4. Close to weakly hydrophobic proteins with positive binding energies ($\Delta G_{eff} > 0$), the membrane thickness is reduced, compared to the bulk: the protein effectively repels the lipids. Strongly hydrophobic proteins with $\Delta G_{eff} \ll 0$ locally compress or expand the membrane depending on the sign of hydrophobic mismatch: the membrane thickness adjusts to the hydrophobic length of the protein in the vicinity of the protein, and relaxes at larger distances.

The thickness profiles were determined as the mean distance between opposing head beads at a given distance $r$ from the proteins. Their shapes can be fitted nicely with an elastic theory originally developed by Safran and coworkers [27–29, 35, 44], shown as solid lines in figure 4. This theory treats the bilayer as a system of coupled elastic monolayers, each having a mean thickness $t_0$, a bending rigidity $k_c/2$, an area compressibility $k_A/2$ and a spontaneous

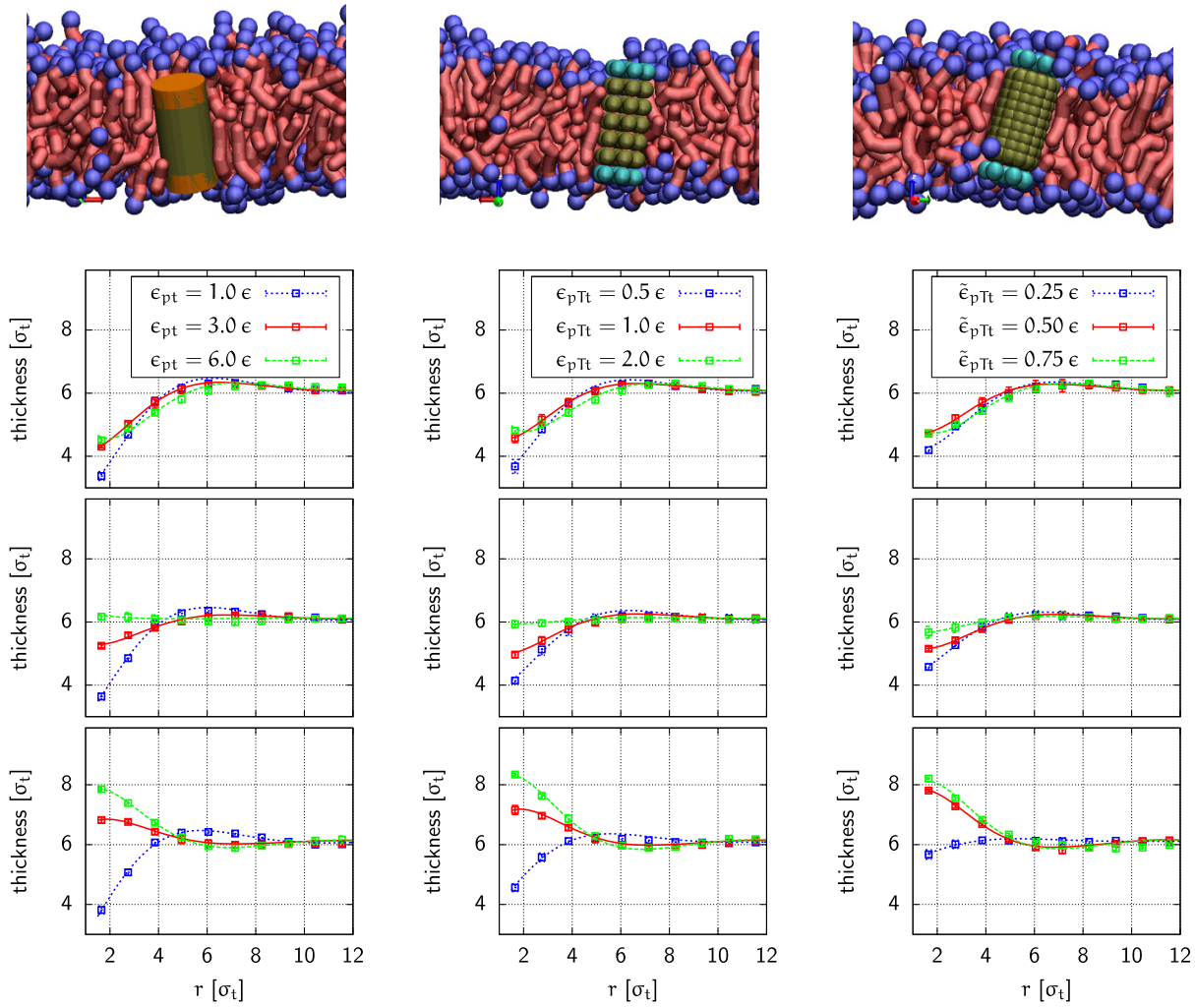


**Figure 4.** Radial bilayer thickness profile around three types of model proteins as indicated. Solid lines show the fit to equations (15) with (17). Left: spherocylinder proteins with hydrophobic length $L = 4\sigma_t$ (top), $L = 6\sigma_t$ (middle) and $L = 8\sigma_t$ (bottom). Middle: rough bead proteins with hydrophobic length $L = 4\sigma_t$ (top), $L = 5\sigma_t$ (middle) and $L = 8\sigma_t$ (bottom). Right: smooth bead proteins with hydrophobic length $L = 4\sigma_t$ (top), $L = 5\sigma_t$ (middle) and $L = 8\sigma_t$ (bottom).

curvature $c_0$. Furthermore, an additional parameter $\zeta$ enters the theory, which is related to the derivative of the spontaneous curvature with respect to the lipid area. The parameters $k_c$, $k_A$ and $\zeta$ have been determined independently for our model bilayers from the fluctuation spectrum, both for tensionless membranes [44] and for membranes under tension [41]. They are given in table 1. The general form of a radially symmetric monolayer thickness profile $\Phi(r) = t(r) - t_0$ reads as [29]

$$\Phi(r) = A_1 J_0(\alpha_+ r) + A_2 Y_0(\alpha_+ r) + A_3 J_0(\alpha_- r) + A_4 Y_0(\alpha_- r) \tag{15}$$

**Table 1.** Elastic constants of our model membrane in Lennard-Jones units as obtained from a fit of the fluctuation spectra of pure membranes to the elastic theory at $\Gamma = 0$ [44] and $\Gamma = 2\epsilon/\sigma_t^2$ [41].

| Parameter | Value at $\Gamma = 0$ | Value at $\Gamma = 2\epsilon/\sigma_t^2$ |
|---|---|---|
| $t_0$ | $3.06 \pm 0.15\ \sigma_t$ | $2.26 \pm 0.08\ \sigma_t$ |
| $k_c$ | $6.2 \pm 0.4\ \epsilon$ | $7.0 \pm 0.3\ \epsilon$ |
| $\zeta/t_0$ | $0.15 \pm 0.09\ \sigma_t^{-2}$ | $-0.038 \pm 0.008\ \sigma_t^{-2}$ |
| $k_A/t_0^2$ | $1.3 \pm 0.3\ \epsilon/\sigma_t^4$ | $1.8 \pm 0.2\ \epsilon/\sigma_t^4$ |

with [44]

$$\alpha_\pm = \sqrt{\frac{2\zeta}{t_0} \pm \sqrt{\left(\frac{2\zeta}{t_0}\right)^2 - \frac{k_A}{k_c t_0^2}}}, \tag{16}$$

where $J_0(x)$ and $Y_0(x)$ are the zeroth-order Bessel functions of the first and second kind, and the parameters $\alpha_\pm$ are complex numbers in stable membranes, $\alpha_\pm = \alpha_r \pm \mathrm{i}\alpha_i$ (with real and positive $\alpha_r, \alpha_i$). Since the profiles must not grow exponentially at infinity, the coefficients $A_i$ fulfil $A_1 =: A$, $A_2 = \mathrm{i}\,A$, $A_3 = A^*$, $A_4 = -\mathrm{i}\,A^*$. The remaining complex coefficient $A$ depends on the boundary conditions at the surface $r = R$ of the protein. For a given surface distortion $\Phi(R) =: t_R$ and surface curvature $\nabla_r^2\Phi|_R =: t_R''$ at the radius $r = R$ (with $\nabla_r^2 = (1/r)\partial_r r \partial_r$), it reads

$$A = \frac{t_R'' + t_R\alpha_-^2}{(\alpha_-^2 - \alpha_+^2)H_0^{(1)}(\alpha_- R)}, \qquad A^* = \frac{t_R'' + t_R\alpha_+^2}{(\alpha_+^2 - \alpha_-^2)H_0^{(1)}(\alpha_+ R)}. \tag{17}$$

The parameters $t_R$ and $t_R''$ are the fit parameters in the theoretical curves of figure 4; they characterize the surface of the protein. More precisely, the theory predicts [35, 44]

$$t_R'' + 2\zeta\frac{t_R}{t_0} = -\left(\frac{k_G}{k_c R}t_R' + 2\tilde{c}_0\right) =: \tilde{C} \tag{18}$$

where $t_R' = \partial_r\Phi|_R$, $k_G$ is the Gaussian curvature and $\tilde{c}_0$ subsumes the effect of the spontaneous curvature $c_0$ as well as possible free-energy contributions from local distortions of other quantities that couple to the membrane thickness [44]. Unfortunately, neither $c_0$ nor $k_G$ can be determined from the fluctuation spectrum. They can be estimated from the moments of the pressure profiles, but the estimate is not very reliable, especially in the case of $k_G$. We will therefore use the parameters $t_R$ and $\tilde{C}$ as defined in equation (18) to characterize the effect of the protein surface on the thickness profiles. In figure 5, we plot the parameter $\tilde{C}$ against the bilayer distortion at the surface. For weakly hydrophobic proteins (leftmost curves), there is no clear dependence. For strongly hydrophobic proteins, however, the curves approach one common line for all protein models. We conclude that the main characteristics of the bilayer thickness profile in the vicinity of strongly bound proteins do not depend on the particularities of the protein model. It is worth noting that the amplitude of the bilayer deformations for the proteins studied here is comparable to that of proteins with fixed upright orientation (as determined in [44]). This is related to the fact that strongly hydrophobic proteins exhibit very little tilt (cf section 3.3).

Another bilayer property that is influenced by a transmembrane protein is the orientation of the lipids. Even though lipid tails are fluctuating and permanently changing their conformation

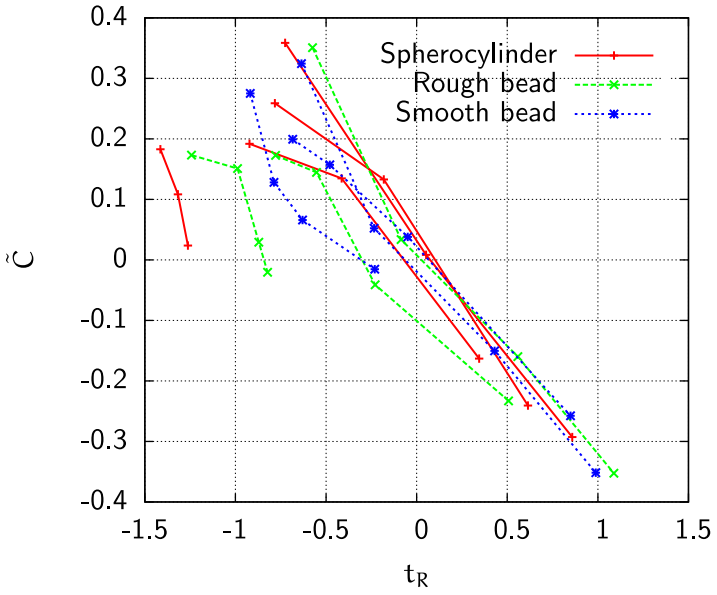


**Figure 5.** Protein surface parameter $\tilde{C}$ versus surface distortion $t_R$ for the different protein models, different hydrophobic strengths and different hydrophobic lengths (cf figure 4): spherocylinders (+) with $L = 4, 6, 8\sigma_t$ and $\epsilon_{pt} = 1, 3, 4, 6$. Rough bead proteins (×) with $L = 4, 5, 6, 8\sigma_t$ and $\epsilon_{pTt} = 0.5, 1, 2$. Smooth bead proteins (stars) with $L = 4, 5, 6, 8\sigma_t$ and $\epsilon_{pTt} = 0.25, 0.5, 0.75$. Lines connect points corresponding to the same hydrophobic strength (which increases from left to right).

within the hydrophobic core of the bilayer, they have average orientations [66], which may be shifted in the presence of a protein. The concept of lipid director has been applied in theories for the lipid-mediated interaction free energies between hydrophobic surfaces [26] and membrane-mediated interaction between two cylindrical inclusions in a symmetric lipid bilayer [32].

Figure 6 shows radial profiles of the average lipid tilt direction for the spherocylinder protein model and for the rough bead protein model. The profiles for positive and negative mismatch are qualitatively different. Close to positively mismatched, strongly hydrophobic proteins, the tilt profile is nonmonotonic: as one approaches the protein, the lipids first tilt towards the protein, then they become straight and may even slightly tilt away from the protein. Lipids near negatively mismatched tilt away from the protein at all distances, but the tilt profiles also become nonmonotonic for strongly hydrophobic proteins, such that the tilt exhibits a maximum at a distance of around $r \sim 4\sigma_t$. This complex behavior is found for both types of protein models. The tilt profiles for the two protein models are almost identical (figure 6).

### *3.3. Orientational distribution of proteins*

Next we examine the orientation distributions of our model proteins in membranes. The orientation of proteins is believed to have a significant influence on their functionality, e.g. in the context of pore formation [67]. Recent coarse-grained simulations have suggested that the cross-angle distributions of packed helix complexes are mostly determined by the tilt angle of individual helices [68]. One important driving force leading to tilt is hydrophobic mismatch

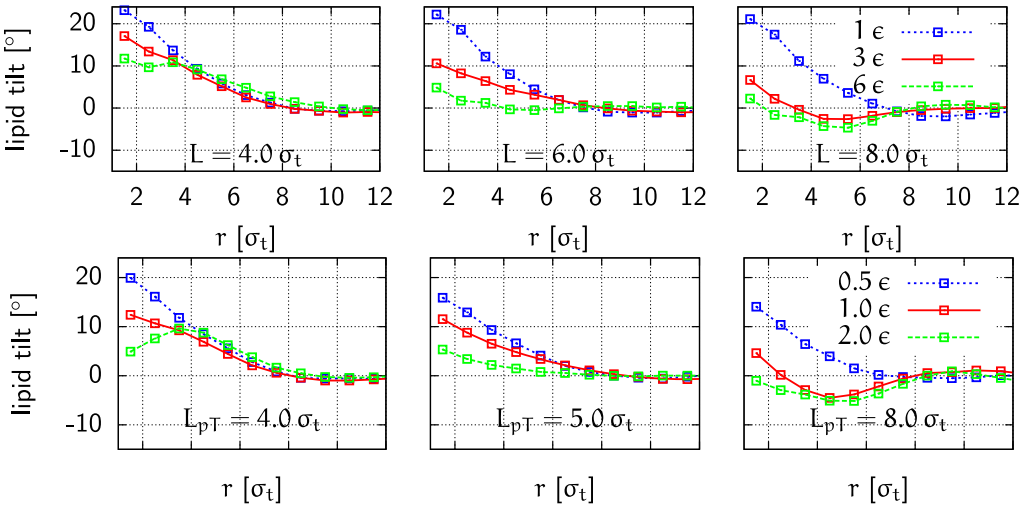


**Figure 6.** Radial profiles of the average lipid tilt with respect to the bilayer normal versus distance $r$ to the center of the protein for spherocylinder proteins (top) and rough bead proteins (bottom) with different hydrophobic lengths as indicated.

[38, 69, 70]. Proteins tilt in order to alleviate the free-energy costs associated with membrane deformations. This is predicted by theoretical considerations [71] as well as molecular dynamics simulations [38, 72, 73].

Experimental tilt measurements, e.g. by nuclear magnetic resonance (NMR) techniques, have in some cases supported this view [69, 74]; in other cases the reported tilt angles were surprisingly small compared to theoretical expectations [75–77]. This has been explained by large orientation fluctuations, which complicate the interpretation of NMR data, especially if peptides are highly mobile [73, 78, 79]. Higher tilt angles are obtained if such fluctuations are taken into account in the analysis [80, 81]. Furthermore, tilt can be influenced by the anchoring residues flanking the hydrophobic transmembrane domains, which have their own preferred orientation at the hydrophobic/hydrophilic interface [70, 82, 83] and might prevent tilting through a variety of mechanisms [76].

Our simulations reveal yet another factor that controls tilt in proteins: the hydrophobicity of the protein. This is demonstrated in figure 7, which shows average tilt angles of different protein models at different hydrophobicities as a function of the relative hydrophobic mismatch $(L - 2t_0)/2t_0$. (We recall that $L$ is the hydrophobic length of the proteins and $2t_0$ the hydrophobic thickness of the membrane.) At negative hydrophobic mismatch or for hydrophobically matched proteins, the average tilt angle takes values around $\langle\alpha\rangle \sim 10^0$, which is in the same range as experimental values [81]. For positively mismatched proteins, the behavior depends markedly on the hydrophobicity of the proteins. In figure 7, the hydrophobicity of the 'weakly hydrophobic' proteins is so small that the binding energy $\Delta G_{\text{eff}} > 0$, i.e. the bound state is thermodynamically metastable only. The tilt angle of such metastably bound proteins increases with increasing positive hydrophobic mismatch as expected. In contrast, strongly hydrophobic proteins with large binding energies, $\Delta G_{\text{eff}} \ll 0$, exhibit average tilt angles which are almost independent of the hydrophobic mismatch and tend to be smaller than those of the corresponding weakly hydrophobic proteins. This result is unexpected and seemingly at

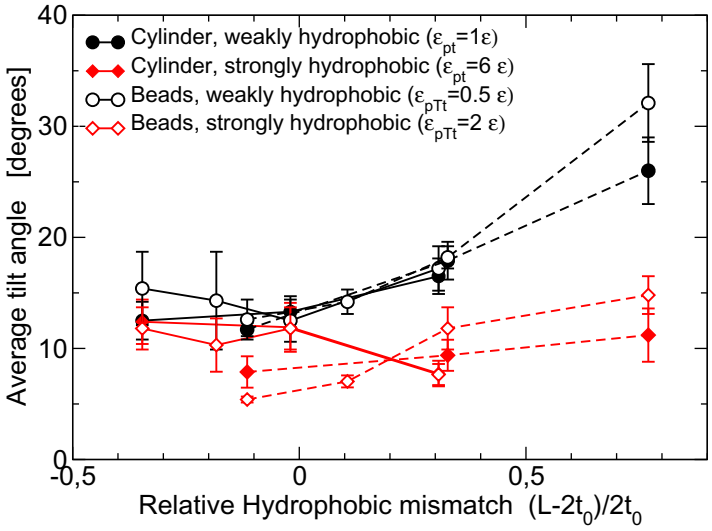


**Figure 7.** Average protein tilt as a function of relative hydrophobic mismatch $(L - 2t_0)/t_0$ in tensionless membranes (solid lines) and in membranes under the tension $\Gamma = 2\epsilon/\sigma_t^2$ (dashed lines), for proteins of different hydrophobic strengths, i.e. weakly hydrophobic proteins in the regime where the bound state is only metastable (circles) and strongly bound proteins (diamonds). Filled symbols correspond to spherocylinders and open symbols to bead proteins.

variance with experimental findings of Özdirekcan *et al* [76], who reported a slight increase of tilt with hydrophobicity. However, it should be noted that the tilt angles reported in this study were generally very small, between 5° and 10°, and the results might be affected by the above-mentioned difficulties of analyzing NMR data for highly mobile peptides.

To analyze this unexpected phenomenon in more detail, we show in figures 8 and 9 a selection of the corresponding orientational distributions. In general, the distributions are very broad, which is consistent with the experimental picture that orientations fluctuate strongly [78, 79, 81]. If one increases the hydrophobic length $L$, the orientational distribution of weakly hydrophobic proteins initially broadens, i.e. more proteins have higher tilt angles. This results in an increased average tilt angle. However, the maximum of the distribution is still found at tilt angle zero. The proteins fluctuate strongly, but their mean position is straight (figure 8). If one increases the positive hydrophobic mismatch even further by applying tension, thus reducing the membrane thickness, a second effect comes into play: the orientation distribution not only broadens further, but also develops a peak at nonzero angle $\alpha$. We conclude that weakly hydrophobic proteins adjust to the membrane thickness by tilting as expected (figure 9).

In the case of strongly hydrophobic proteins, the situation is different. The orientation distribution does not broaden with increasing $L$; instead it sharpens around tilt angle zero, such that longer proteins are on average less tilted than shorter proteins. This behavior is found both for smooth spherocylinder proteins and for bead proteins; hence it seems to be generic. It can be associated with the deformations that strongly hydrophobic proteins induce in the surrounding lipid membrane: the stretched lipids bound to the protein surface stabilize the upright orientation. They order the surrounding lipids, leading to the formation of a dynamic complex consisting of the protein and a lipid shell, which is preferably oriented normal to the

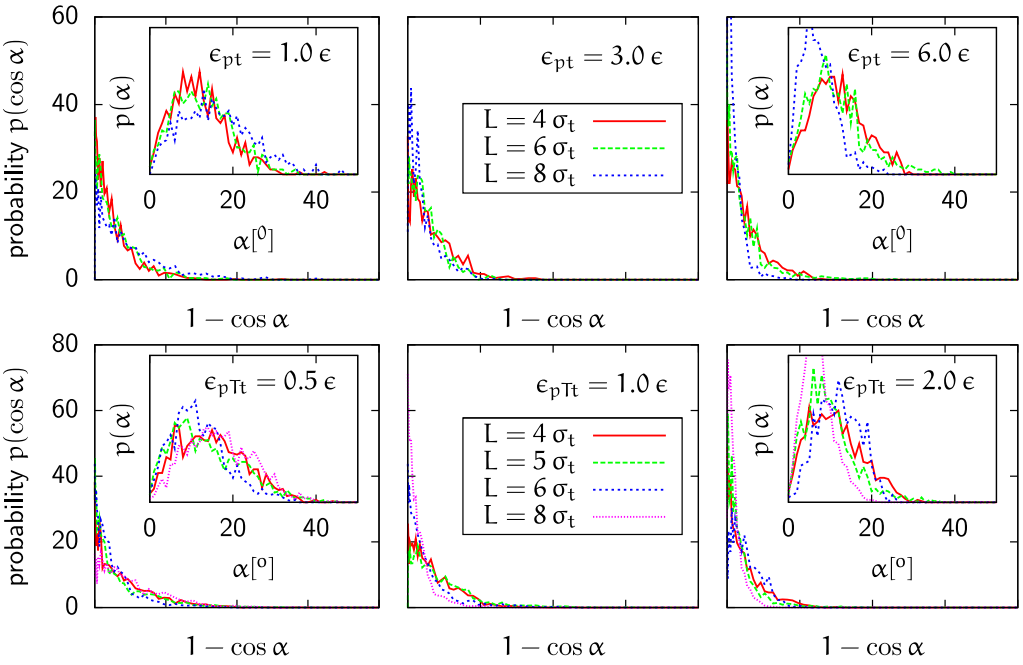


**Figure 8.** Normalized histogram of tilt angles for proteins of different hydrophobic lengths and hydrophobic strengths in tensionless membranes. Here $P(\cos\alpha)\mathrm{d}(\cos\alpha)$ is the number of angles found in the angle interval $\mathrm{d}(\cos\alpha)$. Top row: spherocylinders. Bottom row: rough bead proteins. Insets show the corresponding histograms $P(\alpha)$.

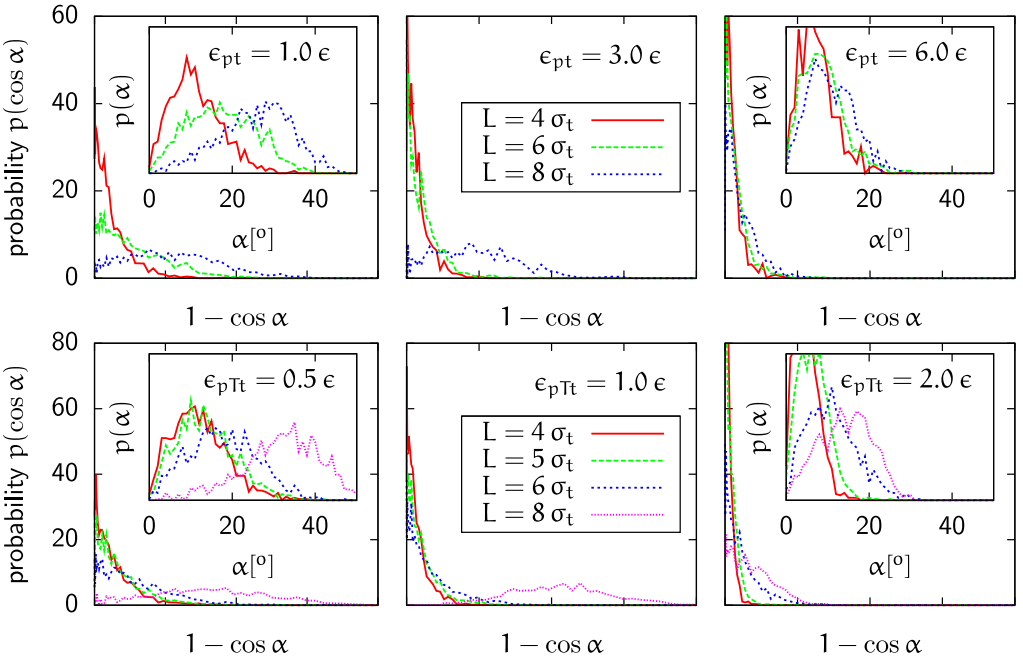


**Figure 9.** The same as figure 8 for membranes subject to the tension $\Gamma = 2\epsilon/\sigma_t^2$.

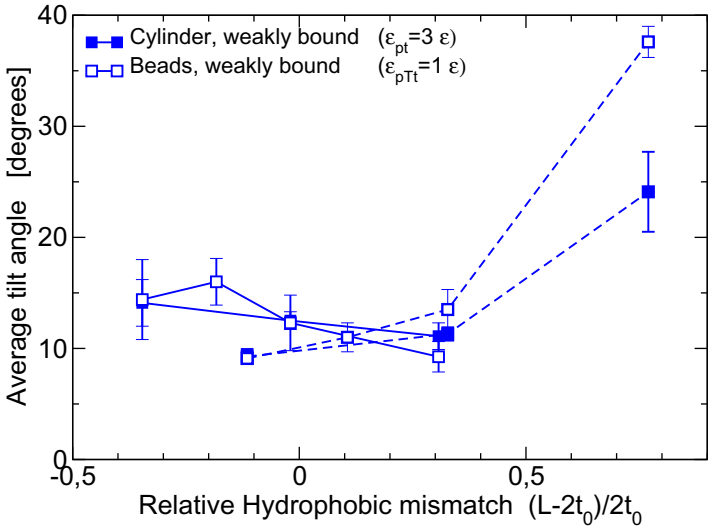


**Figure 10.** The same as figure 7 for weakly bound proteins with intermediate hydrophobic strength.

membrane. A similar effect has been reported for certain model WALP peptides with flanking tryptophane residues [84]. In that case, the anchoring residues were held responsible for the lipid stretching. Apparently, proteins which are capable of inducing significant membrane deformations in their vicinity by whatever mechanism—either due to their hydrophobicity or due to strongly anchoring residues—will tend to form condensed protein–lipid complexes instead of tilting.

Real proteins are in a thermodynamically bound state, but the binding energies are not necessarily very large. Figure 10 shows the behavior of the average tilt for such more realistic proteins as a function of relative hydrophobic mismatch. In this case, the two mechanisms of adjusting to the mismatch compete: as long as the hydrophobic mismatch is small, the protein responds by (slightly) deforming the membrane (cf figure 4) and the surrounding lipids stabilize an upright orientation. If the hydrophobic mismatch becomes large, the protein tilts. Due to the competition, the onset of tilt is not identical with the point where the hydrophobic mismatch turns positive. As a result, the protein behaves as if its hydrophobic length were effectively reduced (figure 10).

To conclude, our simulations suggest that the hydrophobicity of proteins or, more generally, their ability to induce strong membrane deformations plays an important role in determining the tilt. Tilting competes with the formation of dynamic complexes consisting of proteins and their surrounding lipid shells. This second mechanism will be more important if the proteins are more strongly bound in the membrane. We expect that it will also gain importance with increasing protein radius. Most of the systematic experimental studies cited above were based on transmembrane proteins with $\alpha$-helical structure. In our simulations, we have considered proteins with the radius of $\beta$-helices (comparable to gramicidine), which is about three times as thick. Coarse-grained simulations indicate that thicker proteins tilt less than thin proteins [38]. Thus experimental investigations on the interplay of membrane deformation and tilting are presumably more promising if one uses experimental model proteins based on $\beta$-barrels.

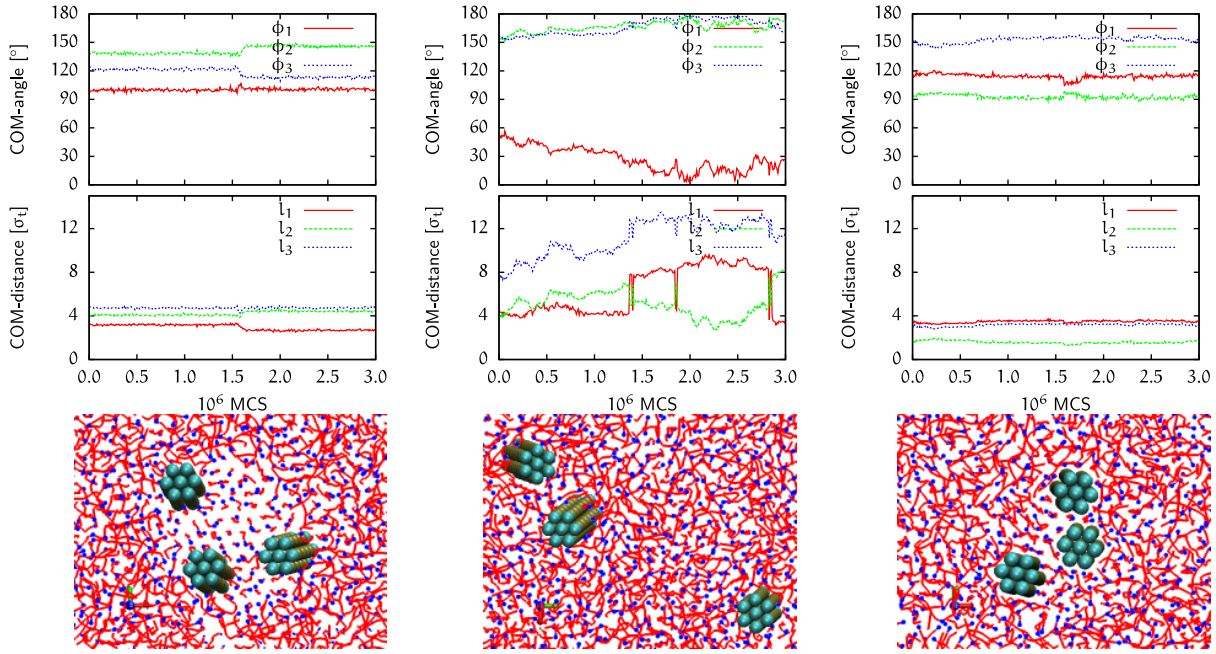


**Figure 11.** Evolution of the COM angles $\phi_i$ and the COM distances $l_i$ during $3 \times 10^5$ MCS for systems containing three moderately hydrophobic rough bead proteins with negative mismatch ($L = 4\sigma_t$, left), no mismatch ($L = 6\sigma_t$, middle) and positive mismatch ($L = 8\sigma_t$, right). The hydrophobicity is $\epsilon_{pTt} = 1\,\epsilon$. Typical configurational snapshots are shown below the graphs.

## 4. Outlook: protein clusters

The next step is to consider membranes that contain several proteins. We have studied the distortion profiles of membranes containing two proteins and, as before, we found no noticeable differences for the different protein models (data not shown, see also the thesis [61]). Membrane-mediated interactions between two proteins have been studied for the spherocylinder model by us [44, 45] and for bead protein models by other authors [85, 86], and the general features are similar. However, it is well known that membrane-mediated protein–protein interactions are not pairwise additive [87]. Many-body effects are important even at low densities. Therefore, we will conclude with a brief discussion of many-body effects. We have studied the time evolution of membranes containing three proteins, which were initially set up on an equilateral triangle with mutual distance $r \sim 6.5\sigma_t$. After equilibration of the system, it was monitored over $3 \times 10^6$ MCS. Quantities used to characterize the orientation of the three proteins with respect to each other are their distance $l_i$ ($i = 1, 2, 3$) from their common center of mass (COM) and the angles $\phi_i$ between the two vectors $\vec{l}_i$ and $\vec{l}_{i+1}$ pointing from the COM to the center of two adjacent proteins (with $\vec{l}_4 \equiv \vec{l}_1$). In the following they will be called COM distances and COM angles, respectively. The angles usually do not give exactly 360° when added up, since we are not measuring the projection of the angles onto the $xy$-plane, but the full angle in space.

Figure 11 shows the corresponding time evolution for rough bead proteins with moderate hydrophobicity. Here we observe a new effect of hydrophobic mismatch which is not yet present

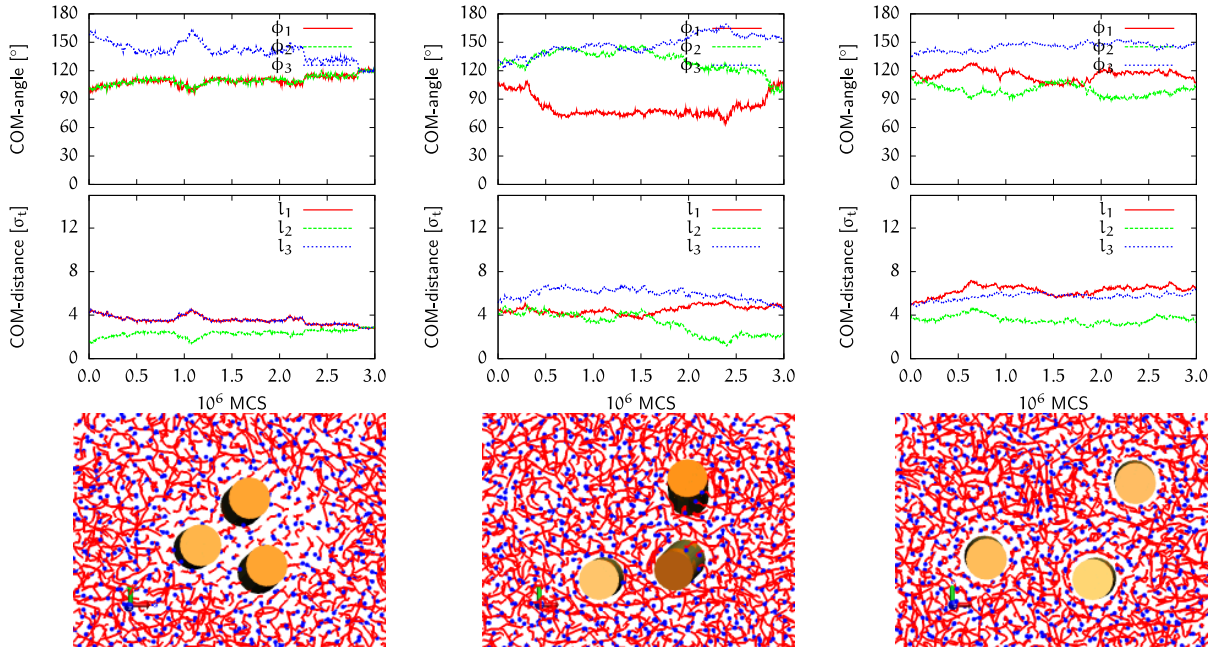


**Figure 12.** The same as figure 11 for strongly hydrophobic spherocylinders with $\epsilon_{pt} = 6.0\,\epsilon$.

in systems containing only one or two proteins. Negatively mismatched proteins may nucleate an ordered lipid state in their direct environment which in turn pins the proteins at their positions, such that they effectively freeze. A similar, albeit weaker, effect is observed for positively mismatched proteins. In contrast, hydrophobically matched rough bead proteins remain mobile and diffuse around slowly during the simulation run.

The onset of a similar effect can be observed for smooth spherocylinder proteins, but only at much higher hydrophobic strengths. For example, if one raises the hydrophobic strength by a factor of 2, clusters of negatively mismatched proteins begin to freeze, but the corresponding positively mismatched cylinders remain mobile (figure 12).

## 5. Summary

In summary, we have studied the influence of the protein on the membrane structure as well as the influence of the membrane on the protein orientations for different protein models. The protein models have in common that they represent rigid cylindrical structures with no internal degrees of freedom. They differ in the degree of roughness of the surface.

For single proteins, we found that the distortion of the lipid bilayer as well as the orientational distribution of the protein are mainly determined by a few generic key parameters such as the hydrophobic length or the strength of the hydrophobic interaction. Details of the protein structure do not matter. Regarding all the quantities considered here, the results for the different protein models with different surface corrugation could be related to each other at an almost quantitative level. The bilayer thickness profiles can be fitted reasonably well for all parameter values with an elastic theory, and the relation between the elastic parameters did not

depend on the protein model. The lipid tilt profiles around the protein as well as the histograms of protein tilt angles were almost identical for the different protein types.

Regarding the protein tilt distribution, we observed an unexpected qualitative difference between weakly and strongly hydrophobic proteins: whereas weakly hydrophobic proteins exhibit strong tilt fluctuations in the membrane, strongly hydrophobic proteins form a complex with the surrounding lipids which keeps them in an upright position. Weakly hydrophobic proteins respond to hydrophobic mismatch by tilting. Strongly hydrophobic proteins remain untilted and distort the membrane. In the biologically most relevant case of moderately hydrophobic proteins that are weakly bound to the membrane (i.e. the hydrophobic strength is just about large enough that the insertion free energy is negative), the two mechanisms compete. Upon increasing the hydrophobic mismatch, the proteins first slightly distort the membrane and then tilt. As a result, their apparent hydrophobic length is reduced. This was observed in all protein models. Overall, the differences between the different protein models were negligible.

We conclude that the microscopic geometric structure has very little influence on the interaction of lipid bilayers with single proteins. The particular choice of the protein model is not very critical as long as one is mainly interested in generic features. However, this changes when looking at systems containing several proteins. In systems containing three hydrophobically mismatched rough bead proteins, we have observed trimerization through the nucleation of an ordered membrane domain. For smooth spherocylinder proteins, this effect was much weaker and only observed for strongly hydrophobic, negatively mismatched proteins. Thus the specific choice of the protein model becomes important if one wants to study complexes of lipids and several proteins. Translating this finding to experimental situations, we would expect the behavior and structure of lipid–protein complexes containing several proteins to be sensitive to details of the protein surface structure even in systems where the characteristics of single protein constituents (i.e. simple $\alpha$-helices or $\beta$-barrels) are mostly determined by generic factors such as hydrophobic mismatch.

The observation that hydrophobically mismatched proteins can nucleate ordered domains with reduced mobility might be interesting in the context of the current raft discussion. We emphasize that these ordered structures have no thermodynamically stable membrane phase counterpart in the absence of proteins. As mentioned in the introduction, the role of proteins in raft formation (if they exist) is not yet clear. Our results indicate that multibody hydrophobic mismatch interactions might provide a possible mechanism that stabilizes rafts. This mechanism should become even more efficient if an ordered lipid phase is close by in parameter space. Similar mechanisms could also stabilize 'liquid ordered' domains with enhanced thickness in mixed membranes even in parameter regions where the liquid ordered state does not represent a distinct thermodynamically stable phase in the pure lipid membrane [88]. Future studies of model membranes containing many proteins in varying lipid environments should shed light on these issues.

## Acknowledgments

This work was funded in part by the German Science Foundation within the Collaborative Research Centres SFB 613 and SFB 625. The configurational snapshots were visualized using VMD [89]. The computer simulations were carried out at the HLRS (Stuttgart) and NIC (Jülich).

## References


[1] Alberts B, Johnson A, Lewis J, Raff M, Roberts K and Walter P 2002 *Molecular Biology of the Cell* (New York: Garland Science)

[2] Gennis R B 1989 *Biomembranes, Molecular Structure and Function (Springer Advanced Texts in Chemistry)* (Berlin: Springer)

[3] Berg J M, Tymoczko J L and Stryer L 2002 *Biochemistry* 5th edn (San Francisco: Freeman)

[4] Singer S J and Nicolson G L 1972 The fluid mosaic model of the structure of cell membranes *Science* **174** 720–31

[5] Vereb G, Syöllösi J, Nagy P, Farkas T, Vigh L, Matyus L and Waldmann T A 2003 Dynamic, yet structured: the cell membrane three decades after the Singer–Nicolson model *Proc. Natl Acad. Sci. USA* **100** 8053–8

[6] Heimburg T 2007 *Thermal Biophysics of Membranes* (New York: Wiley)

[7] Jacobson K, Sheets E D and Simson R 1995 Revisiting the fluid mosaic model of membranes *Science* **268** 1441–2

[8] Sheets E D, Lee G M, Simson R and Jacobson K 1997 Transient confinement of a glycosylphosphidylinositol-anchored protein in the plasma membrane *Biochemistry* **36** 12449–58

[9] Dietrich C, Zant B, Fujiwara T, Kusumi A and Jacobson K 2002 Relationship of lipid rafts to transient confinement zones detected by single particle tracking *Biophys. J.* **82** 274–84

[10] Fujiwara T, Ritchie K, Murkoshi H, Jacobson K and Kusumi A 2002 Phopsholipids undergo hop diffusion in compartmentalized cell membrane *J. Cell Biol.* **157** 1071–81

[11] Daumas F, Destainville N, Millot C, Lopez A, Dean D and Salome L 2003 Confined diffusion without fences of a g-protein-coupled receptor as revealed by single particle tracking *Biophys. J.* **84** 356–66

[12] Douglass A D and Vale R D 2005 Single-molecule microscopy reveals plasma membrane microdomains created by protein–protein networks that exclude or trap signalling molecules in T cells *Cell* **121** 937–50

[13] Pike L J 2006 Rafts defined. A report on the Keystone Symposium on Lipid Rafts and Cell Function *J. Lipid Res.* **47** 1597–8

[14] Jacobson K, Mouritsen O G and Anderson R G 2007 Lipid rafts: at a crossroad between cell biology and physics *Nature Cell Biol.* **9** 7–14

[15] Leslie M 2011 Do lipid rafts exist? *Science* **334** 1046–7

[16] Venturoli M, Sperotto M M, Kranenburg M and Smit B 2006 Mesoscopic models of biological membranes *Phys. Rep.* **437** 1–54

[17] May S 2000 Theories on structural perturbations of lipid bilayers *Curr. Opin. Colloid Interface Sci.* **5** 244–9

[18] Gil T, Ipsen J H, Mouritsen O G, Sabra M C, Sperotto M M and Zuckermann M J 1998 Theoretical analysis of protein organization in lipid membranes *Biochim. Biophys. Acta* **1376** 245–66

[19] Sperotto M M, May S and Baumgaertner A 2006 Modelling of proteins in membranes *Chem. Phys. Lipids* **141** 2–29

[20] Schmid F 2009 Toy amphiphiles on the computer: what can we learn from generic models? *Macromol. Rapid Commun.* **30** 741–51

[21] Mouritsen O G and Bloom M 1993 Models of lipid–protein interactions in membranes *Annu. Rev. Biophys. Biomol. Struct.* **22** 145–71

[22] Ben-Shaul A, Ben-Tal N and Honig B 1996 Statistical thermodynamic analysis of peptide and protein insertion into lipid membranes *Biophys. J.* **71** 130–7

[23] Lagüe P, Zuckermann M J and Roux B 1998 Protein inclusion in lipid membranes: a theory based on the hypernetted chain integral equation *Faraday Discuss.* **111** 165–72

[24] Lagüe P, Zuckermann M J and Roux B 2000 Lipid-mediated interactions between intrinsic membrane proteins: a theoretical study based on integral equations *Biophys. J.* **79** 2867

[25] Lagüe P, Zuckermann M J and Roux B 2001 Lipid-mediated interactions between intrinsic membrane proteins: dependence on protein size and lipid composition *Biophys. J.* **81** 276

[26] May S and Ben-Shaul A 2000 A molecular model for lipid-mediated interaction between proteins in membranes *Phys. Chem. Chem. Phys.* **2** 4494–502
[27] Dan N, Pincus P and Safran S A 1993 Membrane-induced interactions between inclusions *Langmuir* **9** 2768–71
[28] Dan N, Berman A, Pincus P and Safran S A 1994 Membrane-induced interactions between inclusions *J. Physique* II **4** 1713
[29] Aranda-Espinoza H, Berman A, Dan N, Pincus P and Safran S 1996 Interaction between inclusions embedded in membranes *Biophys. J.* **71** 648
[30] Fournier J-B 1998 Coupling between membrane tilt-difference and dilation: a new 'ripple' instability and multiple crystalline inclusion phases *Europhys. Lett.* **43** 725–30
[31] Fournier J-B 1999 Microscopic membrane elasticity and interactions among membrane inclusions: interplay between the shape, dilation, tilt and tilt-difference modes *Eur. Phys. J.* B **11** 261–72
[32] Bohinc K, Kralj-Iglic V and May S 2003 Interaction between two cylindrical inclusions in a symmetric lipid bilayer *J. Chem. Phys.* **119** 7435–44
[33] Fosnaric M, Iglic A and May S 2006 Influence of rigid inclusions on the bending elasticity of a lipid membrane *Phys. Rev.* E **74** 051503
[34] Brannigan G and Brown F L H 2006 A consistent model for thermal fluctuations and protein-induced deformations in lipid bilayers *Biophys. J.* **90** 1501
[35] Brannigan G and Brown F L H 2007 Contributions of Gaussian curvature and nonconstant lipid volume to protein deformation of lipid bilayers *Biophys. J.* **92** 864–76
[36] May E R, Narang A and Kopelevich D I 2007 Role of molecular tilt in thermal fluctuations of lipid membranes *Phys. Rev.* E **76** 021913
[37] Nielsen S O, Ensing B, Ortiz V, Moore P B and Klein M L 2005 Lipid bilayer perturbations around a transmembrane nanotube: a coarse grain molecular dynamics study *Biophys. J.* **88** 3822
[38] Venturoli M, Smit B and Sperotto M M 2005 Simulation studies of protein-induced bilayer deformations and lipid-induced protein tilting, on a mesoscopic model for lipid bilayers with embedded proteins *Biophys. J.* **88** 1778
[39] Guigas G and Weiss M 2006 Size-dependent diffusion of membrane inclusions *Biophys. J.* **91** 2393–8
[40] Reynwar B J, Illya G, Harmandaris V A, Müller M M, Kremer K and Deserno M 2007 Aggregation and vesiculation of membrane proteins by curvature-mediated interactions *Nature* **447** 461
[41] Neder J, West B, Nielaba P and Schmid F 2010 Coarse-grained simulations of membranes under tension *J. Chem. Phys.* **132** 115101
[42] Schmid F, Düchs D, Lenz O and West B 2007 A generic model for lipid monolayers, bilayers and membranes *Comput. Phys. Commun.* **177** 168–71
[43] Lenz O and Schmid F 2007 Structure of symmetric and asymmetric 'ripple' phases in lipid bilayers *Phys. Rev. Lett.* **98** 058104
[44] West B, Brown F L H and Schmid F 2009 Membrane–protein interactions in a generic coarse-grained model for lipid bilayers *Biophys. J.* **96** 101–15
[45] Neder J, Nielaba P, West B and Schmid F 2011 Membrane-mediated protein–protein interactions: a Monte Carlo study *Curr. Nanosci.* **7** 656–66
[46] Haas F M, Hilfer R and Binder K 1995 Layers of semiflexible chain molecules endgrafted at interfaces: an off-lattice Monte Carlo simulation *J. Chem. Phys.* **102** 2960–9
[47] Stadler C, Lange H and Schmid F 1999 Short grafted chains: Monte Carlo simulations of a model for monolayers of amphiphiles *Phys. Rev.* E **59** 4248
[48] Düchs D and Schmid F 2001 Phase behavior of amphiphilic monolayers: theory and simulation *J. Phys.: Condens. Matter* **13** 4853–62
[49] Lenz O and Schmid F 2005 A simple computer model for liquid lipid bilayers *J. Mol. Liq.* **117** 147–52
[50] West B and Schmid F 2010 Fluctuations and elastic properties of lipid membranes in the gel $L_{\beta'}$ state: a coarse-grained Monte Carlo study *Soft Matter* **6** 1275–80

[51] Langel Ü, Cravatt B F, Gräslund A, von Heijne G, Land T, Niessen S and Zorko M 2010 *Introduction to Peptides and Proteins.* (Boca Raton, FL: CRC Press)
[52] de Planque M R R and Killian J A 2003 Protein–lipid interactions studied with designed transmembrane peptides: role of hydrophobic matching and interfacial anchoring (review) *Mol. Membr. Biol.* **20** 271–84
[53] Wimley W C and White S H 1996 Experimentally determined hydrophobicity scale for proteins at membrane interfaces *Nature Struct. Biol.* **3** 842–8
[54] Bechinger B 1996 Towards membrane protein design: pH-sensitive topology of histidine-containing polypeptides *J. Mol. Biol.* **263** 768–75
[55] Mouritsen O G 2005 *Life—As a Matter of Fat* (*The Frontiers Collection*) (Berlin: Springer)
[56] Killian J A 1998 Hydrophobic mismatch between proteins and lipids in membranes *Biochim. Biophys. Acta* **1376** 401–16
[57] Marsh D 2008 Protein modulations of lipids and vice-versa, in membranes *Biochim. Biophys. Acta* **1778** 1545–75
[58] Bohr H G (ed) 2009 *Handbook of Molecular Biophysics* (Weinheim: Wiley-VCH)
[59] Scott H L and Coe T J 1983 A theoretical study of lipid–protein interactions in bilayers *Biophys. J.* **42** 219–24
[60] West B M L 2008 Lipid–protein interactions in lipid membranes *PhD Thesis* Universität Bielefeld
[61] Neder J 2011 Coarse-grained simulations of membranes under tension and lipid–protein interactions *PhD Thesis* Universität Konstanz
[62] Zhanr S E, Brooks B R and Pastor R W 1995 Computer simulation of liquid/liquid interfaces: I. Theory and application to octane/water *J. Chem. Phys.* **103** 10252
[63] Widom B 1982 Potential-distribution theory and the statistical mechanics of fluids *J. Phys. Chem.* **86** 869–72
[64] Beutler T C, Mark A E, van Schaik R C, Gerber P R and van Gunsteren W F 1994 Avoiding singularities and numerical instabilities in free energy calculations based on molecular simulations *Chem. Phys. Lett.* **222** 529–39
[65] Illya G and Deserno M 2008 Coarse-grained simulation studies of peptide-induced pore formation *Biophys. J.* **95** 4163–73
[66] Watson M C, Penev E S, Welch P M and Brown F L H 2011 Thermal fluctuations in shape, thickness and molecular orientation in lipid bilayers *J. Chem. Phys.* **135** 244701
[67] Strandberg E, Tremouilhac P, Wadhwani P and Ulrich A S 2009 Synergistic transmembrane insertion of the heterodimeric PGLa/magainin 2 complex studied by solid-state NMR *Biochim. Biophys. Acta* **1788** 1667–79
[68] Benjamini A and Smit B 2012 Robust driving forces for transmembrane helix packing *Biophys. J.* **103** 1227–35
[69] Park S H and Opella S J 2005 Tilt angle of a trans-membrane helix is determined by hydrophobic mismatch *J. Mol. Biol.* **350** 310–8
[70] Holt A and Killian J A 2010 Orientation and dynamics of transmembrane peptides: the power of simple models *Eur. Biophys. J.* **39** 609–21
[71] Marsh D 2008 Energetics of hydrophobic matching in lipid–protein interactions *Biophys. J.* **94** 3996–4013
[72] Kandasamy S K and Larson R G 2006 Molecular dynamics simulation of model trans-membrane peptides in lipid bilayers: a systematic investigation of hydrophobic mismatch *Biophys. J.* **90** 2326–43
[73] Esteban-Martin S and Salgado J 2007 The dynamic orientation of membrane-bound peptides: bridging simulations and experiments *Biophys. J.* **93** 4278–88
[74] Holt A, Koehorst R B M, Rutters-Meijneke T, Gelb M H, Rijkers D T S, Hemminga M A and Killian J A 2009 Tilt and rotation angles of a transmembrane model peptide as studied by fluorescence spectroscopy *Biophys. J.* **97** 2258–66
[75] Harzer U and Bechinger B 2000 Alignment of lysine-anchored membrane peptides under conditions of hydrophobic mismatch: a CD, $^{15}$N and $^{31}$P solid-state NMR spectroscopy investigation *Biochemistry* **39** 13106–14

[76] Özdirekcan S, Rijkers D T S, Liskamp R M J and Killian J A 2005 Influence of flanking residues on tilt and rotation angles of transmembrane peptides in lipid bilayers. A solid-state $^{2}$H NMR study *Biochemistry* **44** 1004–12

[77] Vostrikov V V, Grant C V, Daily A E, Opella S J and Koeppe R E II 2008 Comparison of 'polarization inversion with spin exchange at magic angle' and 'geometric analysis of labeled alanines' methods for transmembrane helix alignment *J. Am. Chem. Soc.* **130** 12584–5

[78] Strandberg E, Esteban-Martin S, Salgado J and Ulrich A S 2009 Orientation and dynamics of peptides in membranes calculated from $^{2}$H-NMR data *Biophys. J.* **96** 3223–32

[79] Grage S L, Strandberg E, Wadhwani P, Esteban-Martin S, Salgado J and Ulrich A S 2012 Comparative analysis of the orientation of transmembrane peptides using solid-state $^{2}$H- and $^{15}$N-NMR: mobility matters *Eur. Biophys. J.* **41** 475–82

[80] Holt A, Lea Rougier L, Reat V, Jolibois F, Saurel O, Czaplicki J, Killian J A and Milon A 2010 Order parameters of a transmembrane helix in a fluid bilayer: case study of a WALP peptide *Biophys. J.* **98** 1864–72

[81] Strandberg E, Esteban-Martin S, Ulrich A S and Salgado J 2012 Hydrophobic mismatch of mobile transmembrane helices: merging theory and experiments *Biochim. Biophys. Acta* **1818** 1242–9

[82] Chiang C S, Shirinian L and Sukharev S 2005 Capping transmembrane helices of mscl with aromatic residues changes channel response to membrane stretch *Biochemistry* **44** 12589–97

[83] Vostrikov V V and Koeppe R E II 2011 Response of gWALP transmembrane peptides to changes in the tryptophan anchor positions *Biochemistry* **50** 7522–35

[84] de Planque M R R, Boots J W P, Rijkers D T S, Liskamp R M J, Greathouse D V and Killian J A 2002 The effects of hydrophobic mismatch between phosphatidylcholine bilayers and transmembrane alpha-helical peptides depend on the nature of interfacially exposed aromatic and charged residues *Biochemistry* **41** 8396–404

[85] de Meyer F J M, Venturoli M and Smit B 2008 Molecular simulations of lipid-mediated protein–protein interactions *Biophys. J.* **95** 1851–65

[86] Schmidt U, Guigas G and Weiss M 2008 Cluster formation of transmembrane proteins due to hydrophobic mismatching *Phys. Rev. Lett.* **101** 128104

[87] Yiannourakou M, Marsella L, de Meyer F and Smit B 2010 Towards an understanding of membrane-mediated protein–protein interactions *Faraday Discuss.* **144** 359–67

[88] Veatch S L, Cicuta P, Sengupta P, Honerkamp-Smith A, Holowka D and Baird B 2008 Critical fluctuations in plasma membrane vesicles *ACS Chem. Biol.* **3** 287–93

[89] Humphrey W, Dalke A and Schulten K 1996 VMD—visual molecular dynamics *J. Mol. Graph.* **14** 33–8